



ELSEVIER

Mathematics and Computers in Simulation 58 (2002) 443–467



MATHEMATICS
AND
COMPUTERS
IN SIMULATION

www.elsevier.com/locate/matcom

Patterns in networks of oscillators formed via synchronization and oscillator death

L.L. Rubchinsky^{a,*}, M.M. Sushchik^a, G.V. Osipov^b

^a *Institute of Applied Physics, Russian Academy of Science, 46 Ulyanov st., 603600 Nizhny Novgorod, Russia*

^b *University of Nizhny Novgorod, 23 Gagarin Ave., 603600 Nizhny Novgorod, Russia*

Abstract

Pattern formation via synchronization and oscillator death is considered in networks of diffusively coupled limit-cycle oscillators. Different examples of patterns and their dynamics are presented including nontrivial effects such as: (i) synchronized clusters induced by disorder and (ii) transitions from non-propagation to propagation of fronts via the intermittency. © 2002 IMACS. Published by Elsevier Science B.V. All rights reserved.

Keywords: Network of oscillators; Synchronization; Oscillator death; Patterns; Intermittency

1. Introduction

A growing interest in investigations of the dynamics of ensembles of self-excited oscillators is stimulated by the importance of these investigations for the solution of fundamental problems of nonlinear physics such as, for example, pattern formation and the emergence of low-dimensional chaos in multi-dimensional systems [1–3], as well as for the analysis of specific physical phenomena. Such ensembles are frequently encountered in physics, engineering, chemistry, biology, and other branches of science. Modern applications include chains of lasers, Josephson junctions, and relativistic magnetrons, as well as modeling of the mechanisms of rhythmic activity of the cardiac and nervous systems (see, e.g. the literature cited in [4,5]). In recent years, this interest has also been associated with advances made in constructing information processing systems consisting of a large number of active elements (CNN — cellular neural networks [6]).

In the present paper, we will focus on those features of spatio-temporal dynamics of large ensembles of oscillators that significantly depend on synchronization effects. In particular, we will consider in detail patterns whose formation is connected with the so-called oscillator death (amplitude death), when, after breakdown of synchronization, a sufficiently strong dissipative coupling becomes equivalent to additional

* Corresponding author.

E-mail addresses: lrubchinsky@ucdavis.edu (L.L. Rubchinsky), sushch@appl.sci-nnov.ru (M.M. Sushchik), osipov@hale.appl.sci-nnov.ru (G.V. Osipov).

¹ Present address: Center for Neuroscience, University of Californin-Davis, 1544 Newton Ct., Davis, CA 95616, USA.

damping for each interacting oscillator. In the case of inhomogeneous frequency mismatch or pronounced edge effects, the synchronization breaks down locally, which leads to formation of fronts and localized structures. If the frequency of the oscillations depends on their amplitude, this mechanism may give rise to formation of localized structures in two coupled chains even in the absence of edge effects and inhomogeneities of frequency mismatch along the chains [7].

Let us review the basics of this phenomenon in a simple, yet generic example of two coupled limit-cycle oscillators with different frequencies $\omega_{1,2}$:

$$\dot{z}_1 = i\omega_1 z_1 + (p - |z_1|^2)z_1 + d(z_2 - z_1) \quad (1)$$

$$\dot{z}_2 = i\omega_2 z_2 + (p - |z_2|^2)z_2 + d(z_1 - z_2),$$

where $z_{1,2} = |z_{1,2}| \exp(i\phi_{1,2})$ are slow complex amplitudes with phases $\phi_{1,2}$.

Depending on the qualitative properties of the solutions, one can distinguish in the bifurcation diagram three main regions (see Fig. 1): (1) the region of oscillator death in which a trivial solution is stable (we recall that we consider the case when the self-excitation condition $p > 0$ is fulfilled for the uncoupled oscillators); (2) the synchronization region $\dot{\phi}_1 = \dot{\phi}_2$, where the frequencies of the slowly varying amplitudes coincide; and (3) the region of nonsynchronized oscillations $\lim_{T \rightarrow \infty} T^{-1}(\phi_1 - \phi_2) \neq 0$, where the phase difference is unbounded. The transition between regions 2 and 3 has a complicated structure, with both regularly and chaotically modulated oscillations possible in a general case. The transitions between regions 1 and 2 or 1 and 3 are much simpler and are determined from analyses of the stability of the trivial solution. For the system of two oscillators, the eigenvalues for small perturbations are equal to

$$\lambda_{1,2} = p - d \pm \sqrt{d^2 - (\Delta/2)^2},$$

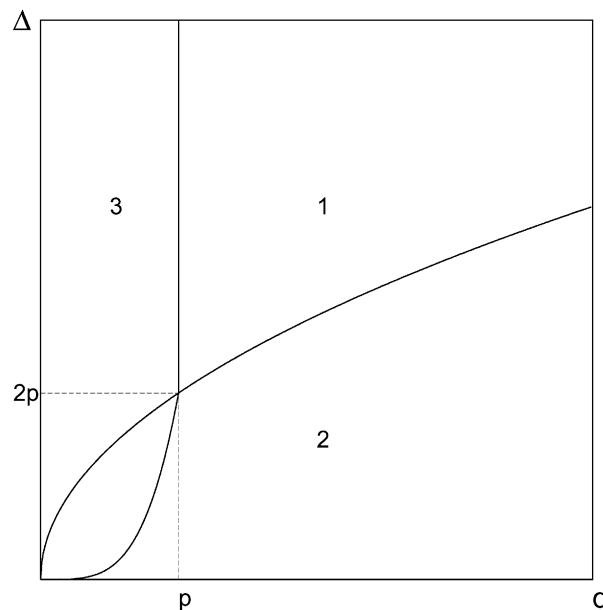


Fig. 1. Bifurcation diagram for a system of two coupled oscillators: (1) region of oscillator death where a trivial solution is stable; (2) region of synchronization; and (3) region of nonsynchronized oscillations.

where $\Delta = \omega_2 - \omega_1$ is the frequency difference of the oscillators. In this case, a transition to a double-frequency regime occurs if $d = p$, $\Delta > 2d$, and to a single-frequency regime if $d = (\Delta^2/4 - p^2)/2p$, $\Delta < 2d$ (Fig. 1).

The following interpretation of oscillator death may be useful. Consider a linearized equation for one of the oscillators:

$$\dot{z}_2 = i\Delta z_2 + pz_2 + d(z_1 - z_2).$$

Here, the term containing the oscillation amplitude of the first oscillator dz_1 , on breaking of synchronization, may be regarded as a nonresonant external force, and the second term that depends on the magnitude of coupling $-dz_2$ exerts the same effect as additional losses. If the losses do not exceed the amplification ($d < p$), a double-frequency regime is possible. For $d > p$, there remain only forced oscillations with an amplitude $\rho_2 = d/|i\Delta + p - d|$ that decreases as the mismatch Δ is increased.

The phenomenon of oscillator death has attracted the attention of researchers probably since the appearance of the papers by Bar-Eli [8,9] (see also [10–12]). A significant progress was achieved in theoretical and numerical analysis of oscillator death in systems of oscillators with “all-to-all” coupling [4,11,13,14]. In recent years, oscillator death has become an object of experimental study [15,16].

The purpose of the present paper is to consider oscillator death and localized structures in two paradigmatic systems: a chain of limit-cycle oscillators with inhomogeneous distribution of natural frequencies along the chain (Section 2), and two coupled homogeneous chains with the frequency of the oscillations depending on their amplitude (Section 3). Our investigations reveal a number of nontrivial phenomena such as cluster synchronization induced by disorder and transitions from non-propagating to propagating fronts via intermittency.

2. Inhomogeneous chains

2.1. Model

In this paper, we restrict ourselves to considering a one-dimensional chain of diffusively coupled oscillators with free ends and linear variation of frequency along it. Such a model was chosen for the following reasons. On the one hand, this model provides a rather broad range of parameters in which synchronized clusters co-exist with regions of oscillator death as is typical of inhomogeneous systems. On the other hand, the model contains the simplest type of inhomogeneities in the sense that, in the limit when the phase approximation [17] is valid, this system, with end effects neglected, becomes homogeneous because the meaningful parameter in this limit is not the frequency but the frequency difference between neighboring elements. This simplicity allows us in a number of cases to obtain the simplest scaling approximations and formulate fairly general results employing a limited number of numerical solutions [18].

In addition, analysis of such chains is of independent interest because they arise in a natural manner when phenomena observed in real life are modeled. Two most instructive examples are the dynamics of the small intestine of mammals and vortex shedding in a flow behind cone-shaped bodies (e.g. supports or chimneys). It is known that if the mammalian small intestine is divided into sections of 1–3 cm long, then each of them is able of oscillating at a definite frequency that changes along the intestine almost linearly over large enough distances [19]. Studies of the vortex shedding in a flow behind cone-shaped bodies also involves analysis of chains of coupled oscillators with linearly varying natural frequencies, if

derivatives with respect to the coordinate along the cone axis are replaced by finite differences (see, e.g. [20]).

Consideration of inhomogeneous chains is carried out on an example of chains of oscillators whose dynamics in a quasiharmonic approximation is described by the discrete analog of the complex Ginzburg–Landau equation for slow complex amplitudes $z_j = |z_j|\exp(i\varphi_j)$ [18,21]:

$$\dot{z}_j = i\omega_j z_j + (p - |z_j|^2)z_j + d(z_{j+1} - 2z_j + z_{j-1}), \quad j = 1, \dots, N, \quad (2)$$

with the boundary conditions $z_1 = z_0$; $z_{N+1} = z_N$ corresponding to a chain with free ends. Without loss of generality we can suppose that $\omega_1 = 0$. In subsequent numerical experiments we set $p = 0.5$, and the number of oscillators $N = 100$. The distribution of natural frequencies along the chain is taken in the form

$$\omega_j = \Delta \frac{j-1}{N-1}. \quad (3)$$

Introduction of different types of inhomogeneities, superimposed on the linear trend, is considered further in the section.

If the values of the frequency gradient along the chain Δ and of the coupling d in Eqs. (2) and (3) are relatively small, a regime of global synchronization is realized. With increasing frequency mismatch Δ and decreasing coupling d well pronounced and rather extended plateaus or steps that are intermittent with a relatively narrow transition region appear in the dependence of the average local frequencies of oscillations on the spatial coordinate. We characterize this effect as cluster synchronization, where the term cluster denotes a coupled set of oscillators having the same average period T and the corresponding mean frequency $\Omega \sim T^{-1}$, with no demand for a constant phase difference between the elements and with allowance for limited variations over time.

Theoretical investigations of cluster synchronization in arrays with linear frequency variations have been carried out for a long time, including modeling the specific behavior of mammalian small intestine [19,22,23]. The problem was formulated and analyzed in the general context in [24] within the framework of the phase equation. However, amplitude effects can be essential in some cases, for example, for the formation and restructuring of cluster structures. A vivid manifestation of these effects is oscillatory death, that occurs at sufficiently strong dissipative coupling in regions of fast increase (or decrease) of the natural frequencies along the chain. Regions of vanishing oscillation amplitude are formed, even if the conditions of self-excitation are fulfilled for each element in the absence of coupling [25–28]. The mechanism of formation of such regions is based on increased losses of oscillations in each oscillator under the action of a sufficiently large dissipative coupling after the breakdown of synchronization [18].

2.2. Cluster synchronization

2.2.1. Synchronized clusters for small values of frequency mismatch and coupling

For the globally synchronous regime, amplitude equations in a zero approximation give the same oscillation amplitudes for all elements of the array. Then, a system of linear equations for phases of oscillators can be derived and solved, which finally yields a criterion for the synchronous regime to be stable (see, e.g. [24]):

$$\left| \frac{\Delta N}{8d} \right| < 1. \quad (4)$$

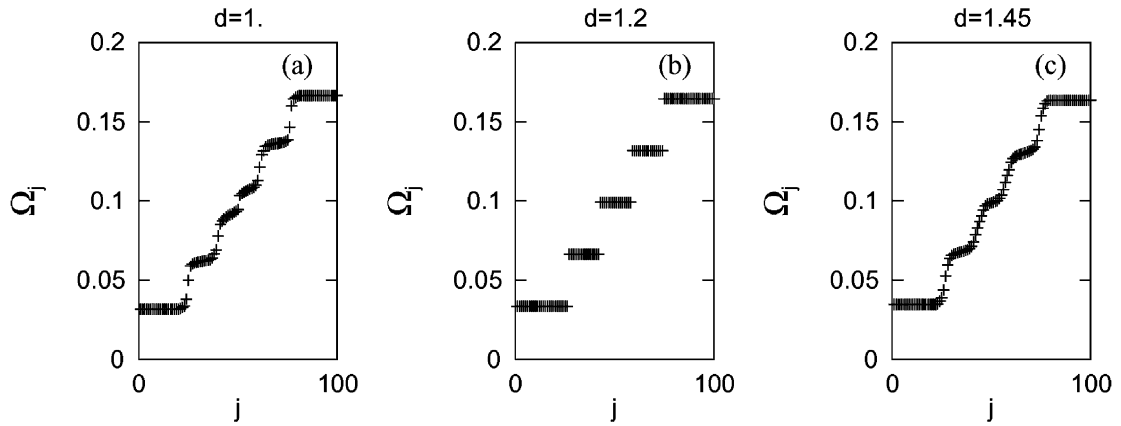


Fig. 2. Averaged frequencies Ω_j and their difference $\Delta\Omega_j = \Omega_{j+1} - \Omega_j$ for perfect and intermediate cluster structures for $\Delta = 0.2$.

For $\Delta \approx 8d/N$, the regime of global synchronization loses stability and for not too large Δ and d two basic regimes are realized, as Δ/d is increased, depending on the specific values of the parameters. The first is the regime of multifrequency generation, where most elements of the array (except, perhaps, the edge ones) generate different frequencies like in Fig. 2(a and c). The second one is the regime of cluster synchronization, where all the oscillators are divided into several groups inside each of which all the elements oscillate at the same average frequency (Figs. 2(b) and 3). The values of frequency for each cluster (except the edge ones) are close to those obtained by averaging natural frequencies over all the elements forming the cluster. In the considered case of a linear dependence of the frequency on j in Fig. 3, this corresponds to the intersection of the lines $\Omega = \Omega_j = \dot{\phi}_j$ and $\Omega = j\Delta/N$ exactly in the middle of

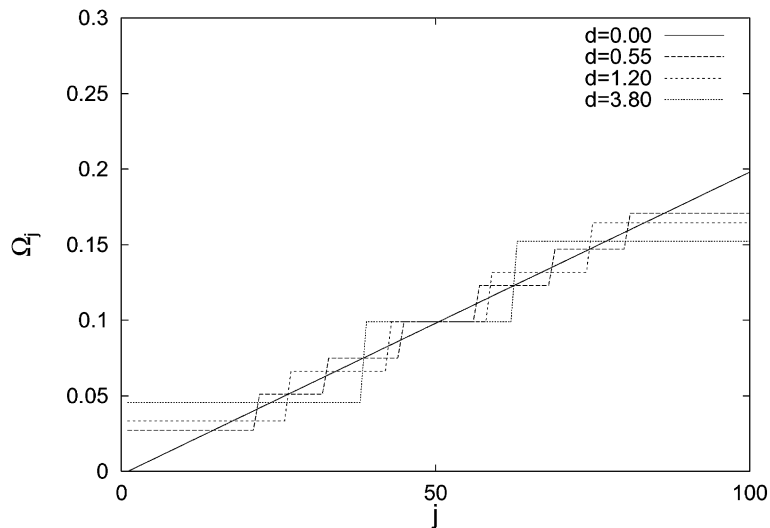


Fig. 3. Averaged frequencies Ω_j for different values of the coupling coefficient d in the case $\Delta = 0.2$.

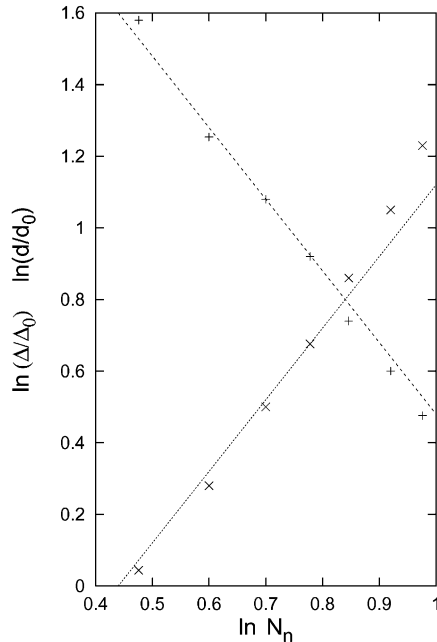


Fig. 4. Critical values of the frequency gradient (x) in the range $\Delta \approx (0.5 - 17) \times 10^{-3}$ for $d = 1$ and of the coupling coefficient (+) in the range $d \approx 0.3 - 3.8$ for $\Delta = 2 \times 10^{-3}$ depending on the size of the middle clusters N_n . The critical values denote the values, at which the n -cluster structure breaks down prior to the transition from the n to the $n + 1$ cluster. The scale is logarithmic to an accuracy of arbitrarily chosen origin; the straight lines correspond to the dependence (6).

the cluster. These cluster structures are periodic in time: the frequency differences between the clusters in such structures coincide and are equal to the lowest cluster frequency

$$\Omega_n = \Delta / (n + 1). \tag{5}$$

The size of the clusters, N_n , for small Δ may be approximated, to an accuracy of ± 1 element, by the relations for the middle clusters:

$$N_n = \frac{N - 1}{n + 1}, \tag{6}$$

and for the edge clusters:

$$N_n = \frac{3}{2} \frac{N - 1}{n + 1}. \tag{7}$$

Here, $N (= 100)$ is the number of elements and $n (= 2, \dots)$ is the number of clusters. The sizes of middle clusters N_n at the instants when they break are plotted in Fig. 4. The scaling by parameters Δ and d is similar to the one that specifies, in the constant amplitude approximation ($|z_j| = |z_0|$), the limiting size of the array with free ends in which the global synchronization (4) may occur:

$$N_n \sim \left(\frac{8d}{\Delta} \right)^{1/2}. \tag{8}$$

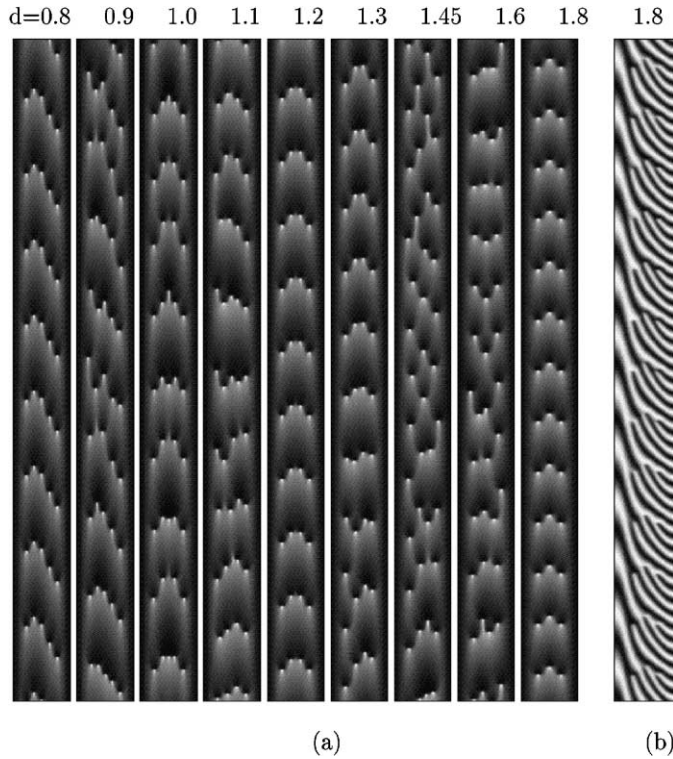


Fig. 5. Space–time diagrams: (a) intensities of $|z_j|^2$ and (b) real parts $\text{Re}(z_j)$ for $\Delta = 0.2$ and different values of the coupling coefficient. The spatial coordinate $j = 1, \dots, 100$ is plotted on the horizontal axis, and time $t \in [0, 4000]$ along the vertical axis.

The spatio-temporal behavior of cluster structures is illustrated in Fig. 5, where the darker regions mark the higher values of intensities of $|z_j|^2$ (Fig. 5(a)) and real parts $\text{Re}(z_j)$ (Fig. 5(b)) of complex amplitudes of oscillations. Oscillograms of intensities for the middle elements of the array are shown in Fig. 6. Detailed comparison of the data given in these figures as well as in Fig. 2 leads to the conclusion that perfect cluster structures may be formed (for $d = 0.8; 1.2; \text{ and } 1.8$ in Figs. 2 and 5).

The intensity of $|z_j|^2$ decays periodically almost to zero at the cluster boundaries (Fig. 6(c)). With increasing distance from the boundary of the clusters, the intensity decreases so that the change of the real part of complex amplitudes z_j in the (j, t) -plane shown in Fig. 5(b) represents correctly the phase of z_j . The formation of a defect in the spatio-temporal pattern of the phase (or $\text{Re}(z_j)$), that is visualized as the singularity of the intensity field of $|z_j|^2$, corresponds to the transition between the clusters.

Since the number of the defects, n_D , formed in one period of a perfect cluster structure is a unity less than the number of clusters n and their repetition rate is $T = 2\pi \Omega_n^{-1}$, the number of the defects per unit time is equal to

$$\rho_D = \frac{n_D}{T} = \frac{\Delta(N - 1)}{2\pi} \frac{n - 1}{n + 1}. \tag{9}$$

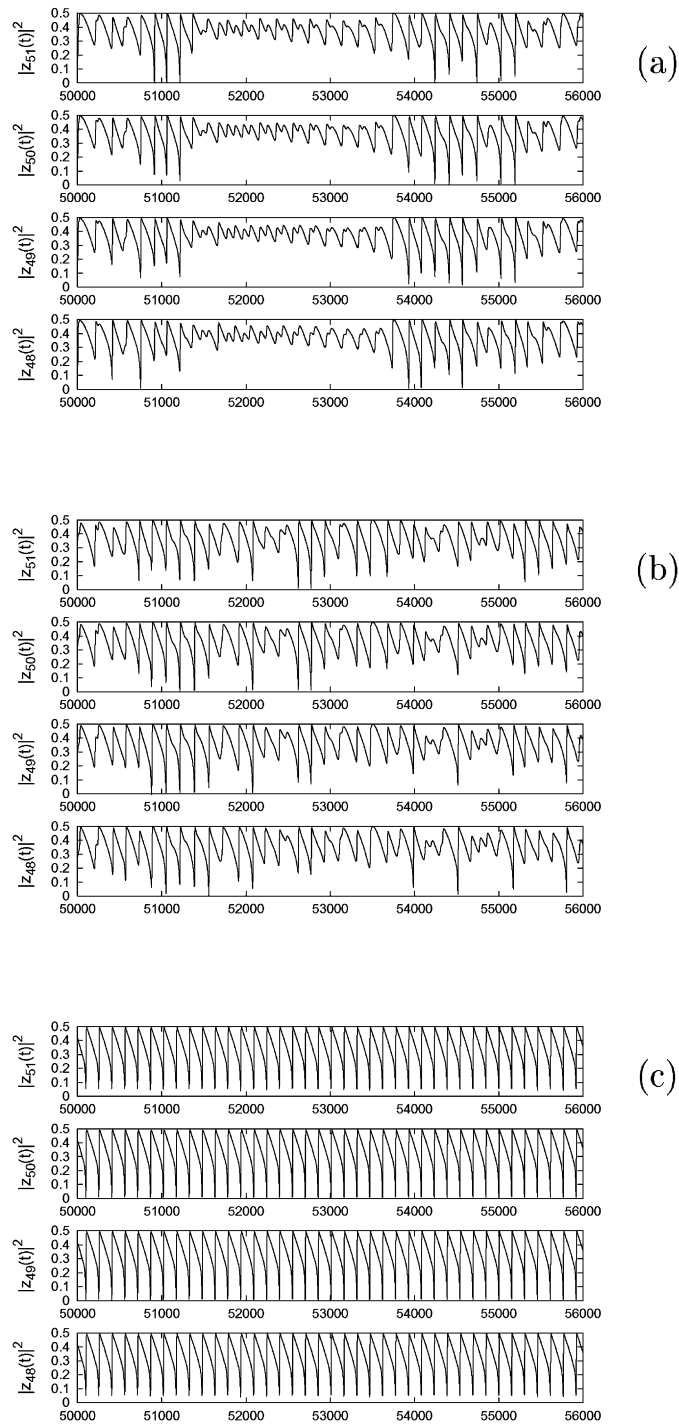


Fig. 6. Intensity oscillograms for the middle elements of the array for $\Delta = 0.2$: (a) $d = 1.45$; (b) $d = 1.65$; and (c) $d = 1.8$.

Estimates by these formulas agree well with the data obtained directly from numerical solutions. In particular, the number of the defects is equal to 44, 40 and 39 for the case shown in Fig. 5(a) at $d = 0.8, 1.2,$ and $1.8,$ and to 45, 42, and 38, respectively, when calculated by the formula (9). Note that, when the transitions between the structures with n and $n + 1$ clusters are caused by changes of the coupling coefficient $d,$ the average defect density changes only slightly at $n \geq 4.$ At the same time, their relative position in the (j, t) -plane alters significantly. For example, in Fig. 6(a) it changes from completely ordered at $d = 1.2$ to irregular at $d = 1.45,$ and then again to a regular one but now with a different symmetry at $d = 1.8.$ The time series undergo the corresponding changes too (see Fig. 6).

Both the picture of synchronization presented above and its description in a rather general form on the basis of numerical solutions are possible due to high degree of symmetry and homogeneity of the problem in a quasiharmonic approximation at small frequency gradients and coupling coefficients. Actually, the meaningful quantity in this approximation is not the frequency itself but the frequency difference $\Delta.$ Consequently, the system may be regarded to be homogeneous if the edge effects are neglected. The picture is becoming more complicated, as Δ and d are increased to make the effects of multistability and the changes of the amplitudes of oscillations along the array essential.

2.2.2. Multistability

Investigations into processes of cluster structure formation revealed multistability, the most vivid manifestation of which is formation of structures containing a different number of clusters depending on initial conditions. The existence domains of structures having a definite number of clusters obtained in numerical experiment with adaptation of the initial conditions to small variations of the parameters are shown in Fig. 7. The adaptation procedure was as follows: The mismatch Δ was varied successively

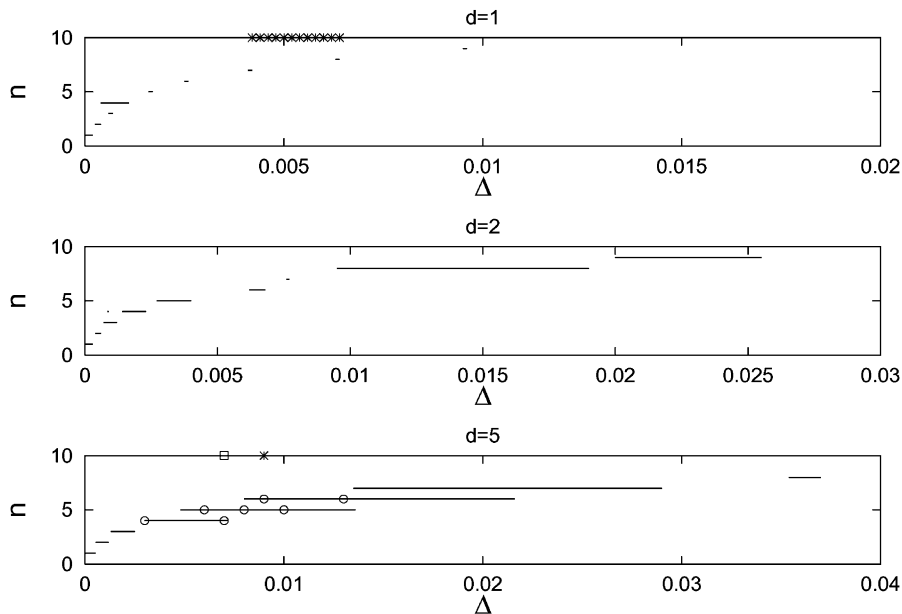


Fig. 7. The ranges of frequency gradients at which structures with n perfect clusters of the type shown in Fig. 2(b) are given for coupling coefficients $d = 1; 2;$ and $5.$

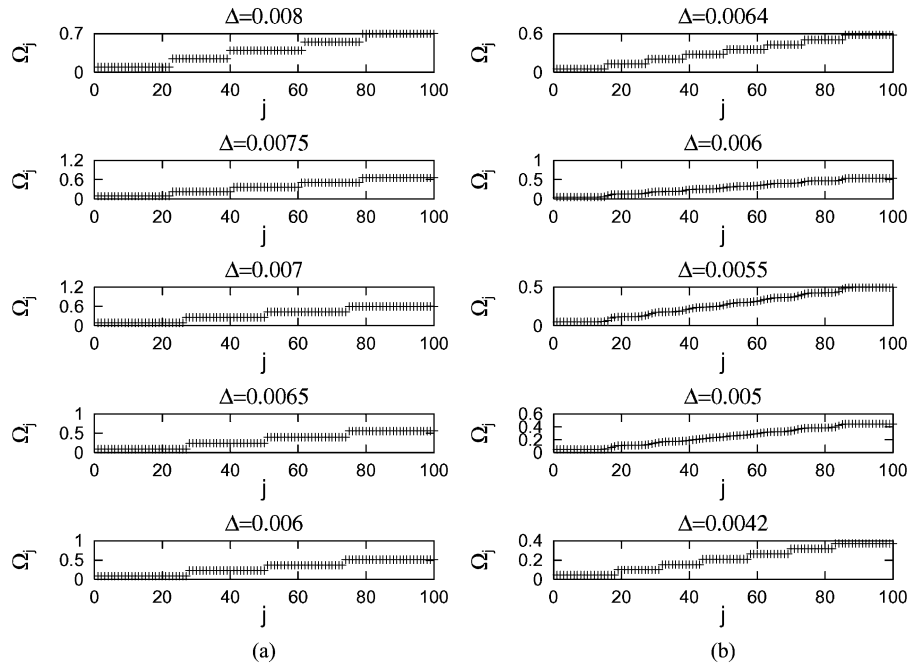


Fig. 8. Averaged frequencies Ω_j in the transitions from n to $n + 1$ clusters: (a) “hard” transition for $d = 5$; (b) “soft” transition for $d = 1$. The corresponding regions of parameters are indicated in Fig. 7 by (○).

by $+5 \times 10^{-4}$ or by -5×10^{-4} . The values from the steady-state solution obtained in the previous variant were taken as the initial conditions for $z_i(t)$. Although the procedure described does not guarantee that all possible regimes will be found, it enables us to reveal qualitatively different transitions in the domain, where the states possessing a different number of clusters co-exist, i.e. in the region of multistability and in the region of parameters where it is absent. In the first case (Figs. 8 and 9(a)), as Δ increases by $<5 \times 10^{-4}$, a “hard” transition without intermediate structures from the state with four clusters to the state with five clusters occurs. In the second case (Fig. 8(b)), a “soft” transition occurs at a much greater interval of variations $\Delta \approx 2.2 \times 10^{-3}$, with a smooth transition of intermediate structures one into another.

Note that a nonmonotonic dependence of the number of clusters on the magnitude of frequency mismatch (Fig. 8) is observed in the region of multistability when solutions under the same initial conditions are sought (in particular, $x_j(0) = -2$ for even j , $x_j(0) = 2$ for odd j , and $y_j(0) = 0$ for all j). This is evidently due to an intricate structure of the basins of the corresponding attractors in phase space, the deformation of which leads to the alternating initial conditions in each of them. This lays the basis for one of the methods of governing the processes of formation of the structures of mutually synchronized elements [28].

The sophisticated structure of the phase portrait of the considered system does not exclude that multistable regimes of other types, when the structure of the clusters rather than their number is changed, may also be observed. For verification of this hypothesis we conducted a series of experiments in which the amplitude and phase distributions formed earlier in the clusters but now with a different number of

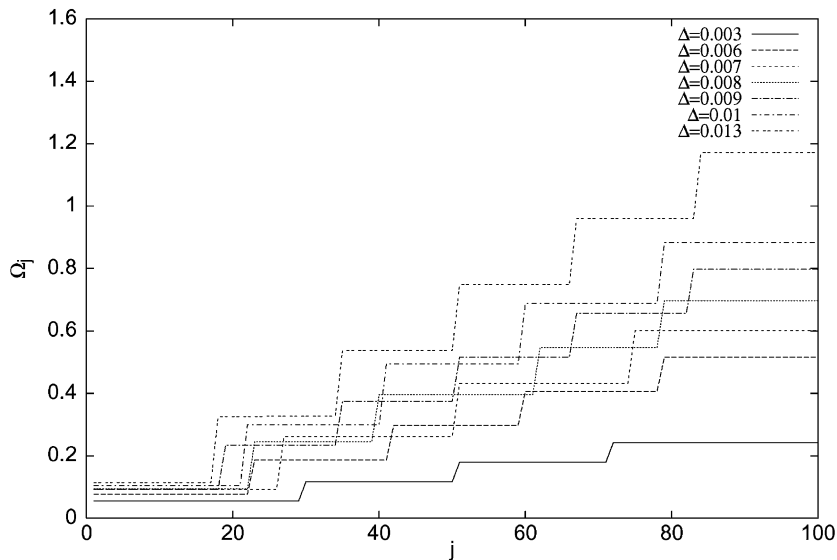


Fig. 9. Nonmonotonic sequence for the number of clusters (4,5,4,5,6,5,6 upwards) under monotonic variation of the frequency gradient Δ and identical initial conditions ($d = 5$). The corresponding values of the parameters are marked in Fig. 7 by (\times).

elements were taken as initial conditions (usually, the number of elements in the cluster was changed by $N_n = \pm 1, 2$). It was found that the same cluster structure was always established in the region of the parameters of interest with such variations of initial conditions.

2.3. The action of disorder on oscillatory death

As we increase Δ and d , oscillator death may appear in the array. In this situation, the oscillator death manifests itself first of all as a formation at the center of the chain of a region in which the oscillation amplitudes vanish. Let us recall again that the oscillator death is associated with the fact that, for a large difference of natural frequencies of neighboring oscillators, the influence of nonresonant terms proportional to z_{j+1}, z_{j-1} in the equation (2) for z_j is relatively weak, and the diffusive coupling introduces damping (the term $-2dz_j$) that exceeds amplification at large d ($d \geq p/2$). For chains with free ends, when the linear frequency trend grows, this effect is manifested first at the center of the chain where desynchronization occurs first with increasing frequency mismatch [18] (Fig. 10).

Here, we are addressing the issue of how spatial disorder introduced to the linear trend of natural frequencies influences oscillatory death in the system [21]. The influence of disorder on dynamics of oscillatory arrays proved to be very nontrivial. The inhomogeneities (including spatially irregular ones, i.e. disorder) introduced into the system in which complex spatio-temporal patterns exist can, for example, lead to more synchronous behavior of the oscillators. Examples include improved synchronization in ensembles of coupled nonlinear pendulums modeling chains of Josephson junctions [29] and in arrays of coupled maps used as models of earthquake dynamics [30], as well as regularization of dynamics in chains of coupled chaotic oscillators [31–33]. However, the influence of spatial disorder on oscillator death in oscillator arrays with local couplings has not previously been analyzed in these works.

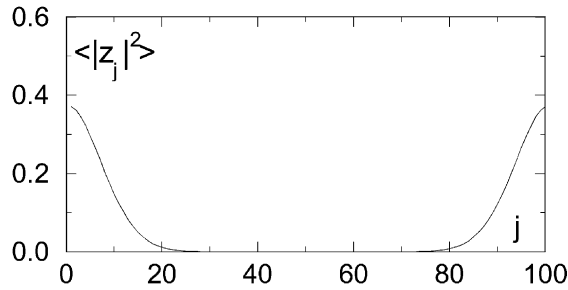


Fig. 10. Oscillator death in the chain with constant frequency gradient. Total frequency range (the difference between the lowest and highest frequencies ω_1 and ω_{100}) is 6.0. Plotted is the time-averaged intensity profile.

Although manifestations of the considered effects in specific applications fall outside the scope of our paper, as qualitative characteristics we choose functionals that can be useful for estimating the action of signals from oscillator chains on some types of sensors. These functionals are the normalized mean “incoherent” energy

$$\varepsilon = \frac{\langle \sum_{j=1}^N |z_j|^2 \rangle}{\langle \sum_{j=1}^N |z_j^{(0)}|^2 \rangle} = \frac{\langle \sum_{j=1}^N |z_j|^2 \rangle}{Np} \tag{10}$$

and normalized mean “coherent” energy

$$w = \frac{\langle |\sum_{j=1}^N z_j|^2 \rangle}{\langle |\sum_{j=1}^N z_j^{(0)}|^2 \rangle} = \frac{\langle |\sum_{j=1}^N z_j|^2 \rangle}{N^2 p}, \tag{11}$$

where $z_j^{(0)}$ are the complex amplitudes of in-phase oscillations excited in the limit of infinitesimal frequency mismatch; $\langle \cdot \rangle$ denotes averaging over time. In the numerical experiments presented in this section we set $d = 10$.

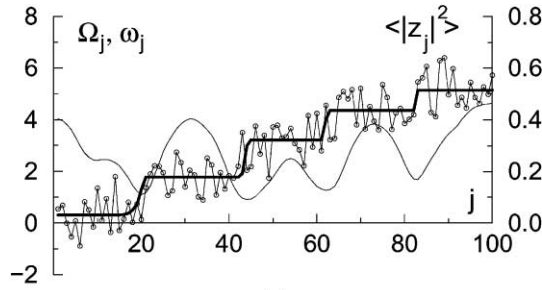
2.3.1. Oscillatory death elimination by disorder

We introduce disorder in a way such that the value of the linear frequency trend Δ and the range of random frequency scatter Δ^* change independently of each other, i.e.

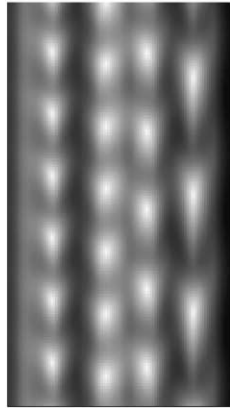
$$\omega_j = \Delta \frac{j-1}{N-1} + \Delta^* \xi_j, \tag{12}$$

where ξ_j are random numbers distributed uniformly in the interval $[-0.5; +0.5]$. As before N is the number of oscillators in the chain.

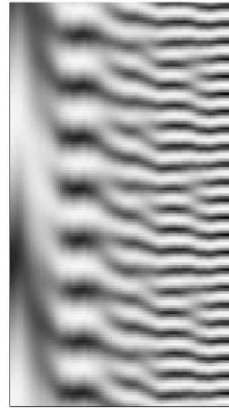
In typical variants of this series, introduction of disorder into distribution of natural frequencies either did not affect significantly oscillator death (“unfavorable” disorder) or resulted in pronounced growth of oscillation amplitudes, so that the region of death diminished appreciably or even vanished (“favorable” disorder). The latter was dominating in the series on the average. Typical examples are represented by spatial distribution of time-averaged oscillation intensities $\langle |z_j|^2 \rangle$ in Fig. 11(a), and by spatio-temporal diagrams for $|z|$ in Fig. 11(b). Fig. 11(c) shows spatio-temporal diagrams for $\text{Im } z_j(t)$ that illustrate the variation of phase in time and space: the variation of the picture from maximally dark to light in the region of smooth variations of amplitude corresponds to the change of phase by π .



(a)



(b)



(c)

Fig. 11. Chain with linear frequency trend and introduced disorder (12), $\Delta = 6.0$ and $\Delta^* = 0.2\Delta$. (a) Time-averaged intensity profile $\langle |z_j|^2 \rangle$ (solid line), averaged frequencies of oscillations Ω_j (bold line), and natural frequencies ω_j (circles connected by dashed line); (b) $x-t$ plot of amplitude $|z_j(t)|$ (time increases upward for 30 units and the position along the array varies horizontally), white corresponds to zero and black to the maximal value of the amplitude, which is about \sqrt{p} ; (c) $x-t$ plot of $Im(z_j(t))$, white and black colors correspond to minimal and maximal values of $Im(z_j(t))$ (about $\pm\sqrt{p}$), respectively.

Mean “incoherent” ε and “coherent” w energies versus the range of random frequency scatter of oscillator natural frequencies relative to the linear trend are plotted in Fig. 12 for different values of the trend (the values of ε and w were obtained by averaging the “incoherent” and “coherent” energies over the ensemble of 25 sets of natural frequencies $\{\omega_j\}_{j=1}^N$ with different samples of disorder). From the data presented in Fig. 12(a) it follows that, for the values of parameters Δ and d corresponding to weak manifestation of the effect of oscillator death $\varepsilon(\Delta^* = 0) \approx 0.6-0.7$ (the curves in Fig. 12(a) for $\Delta = 0.75; 1.5$), introduction of disorder into the frequency distribution does not lead to pronounced changes in the average level of incoherent energy ($\sim 10\%$). However, for Δ and d such that $\varepsilon(\Delta^* = 0) \approx 0.1 \simeq 0.3$, more than a two-fold increase of the incoherent energy can occur when disorder is introduced. It is worthy of noting that this effect is interesting not only from an academic point of view because it is observed at the values of ε that are of practical importance. If the effect is evaluated in comparable frequency gradients, then, as it follows from the data given in Fig. 12(a), introduction of spatial disorder can be equivalent to more than a two-fold decrease of frequency gradient. For example, the oscillator death effect

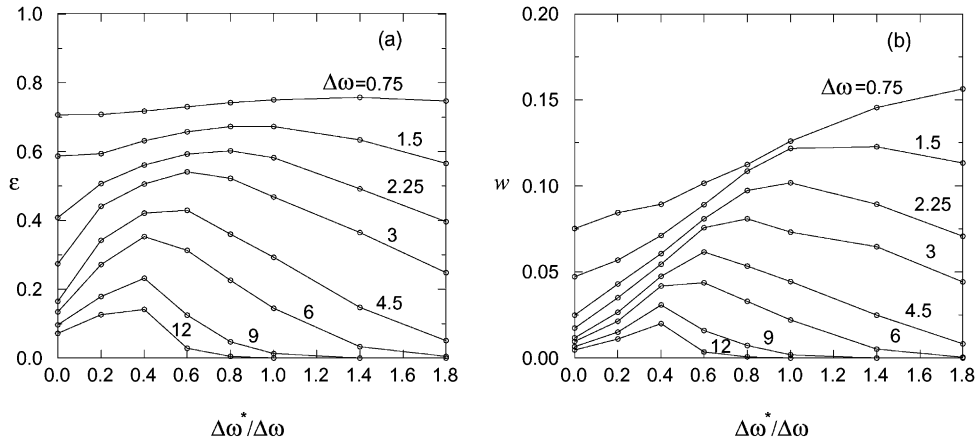


Fig. 12. Dependences of the “coherent” (a) and “incoherent” (b) energies ε and w on the relative level of disorder Δ^*/Δ introduced by the rule (12) for different values of the linear frequency trend Δ .

corresponding to $\varepsilon = 0.3$ for $\Delta = 3.0$ is approximately the same as for $\Delta = 6.0$ but with additionally imposed frequency disorder.

Concerning the “coherent” energy w we can say that, even in the case of complete synchronization in a chain with a linear trend, the value of $\langle |\sum_{j=1}^N z_j|^2 \rangle$ may be much smaller than its maximum $N^2 p$ because of the finite phase difference between oscillations of neighboring oscillators. Consequently, analysis of the normalized value of w is meaningful not only for $w \approx 1$ but for $w \ll 1$ as well. As it follows from the data in Fig. 12(b), in this case introduction of disorder into frequency distribution may have the same effect as a decrease of the large-scale frequency gradient by more than three times. In addition, under the action of disorder w can change in a wider interval than ε . For instance, for the data in Fig. 12(b), introduction of disorder at $\Delta = 2.25$ – 4.5 results in an almost fourfold increase of w .

A distinctive feature of the dependences $\varepsilon = \varepsilon(\Delta^*)$ and $w = w(\Delta^*)$ shown in Fig. 12 is the existence of the optimal value Δ_{opt}^* maximizing ε and w . It is interesting that this optimal value of the frequency band Δ^* characterizing the spread relative to the mean value at each point of the array proved to be comparable to the total range of large-scale (regular) variation of frequency Δ . At least, it is true for the parameter region of practical interest in which $\varepsilon > 0.1$; $w > 1/N$ in the absence of disorder.

2.3.2. Mechanism of disorder influence on oscillator death

A previous study of pattern formation in the system under consideration [18] indicates that there exist at least two mechanisms of the action of introduced disorder on oscillator death. One of them involves a transformation of the attractor (or attractors) as a whole and the other, which is effective in the presence of multistability, implies that the attractors change only slightly, but their attracting basins are transformed. However, it was found that bistability regions occupy only a small portion of parameter space. So, the role of the second mechanism is insignificant, if any. In our case, it could manifest itself only at $\Delta \approx 1$, i.e. at relatively weak oscillator death. However, the difference in the values of “incoherent” energy $\varepsilon(\Delta^* = 0)$ for four-cluster (0.630) and five-cluster (0.628) structures is small and comparable with the changes of their energies under the action of weak disorder without change in the number of clusters. In particular, for $\Delta^* = 0.035$, the values of $\varepsilon(\Delta^* = 0.035)$ are equal to 0.616 and 0.638, respectively.

The action of the first mechanism involving a transformation of the entire cluster structure is demonstrated in Fig 11. It is clear from this figure that favorable situations are possible when disorder gives rise to synchronized clusters with oscillation intensities comparable to those observed in arrays without oscillator death. Formation of such clusters is caused by longwave components in the frequency distribution. Let us explain it by a very simple example, where the superimposed frequency scatter has a purely sinusoidal dependence, so that

$$\omega_j = \Delta \frac{j - 1}{N - 1} + \frac{\Delta^*}{2} \sin \frac{2\pi}{N_\lambda} (j - 1),$$

where N_λ is the spatial period. Apparently, the formed frequency distribution at sufficiently large amplitude of deviations ($\Delta^*/\Delta \geq \pi/N_\lambda$) will have nearly horizontal plateaus, so that $\omega_{j+1} - \omega_j \ll \Delta/(N - 1)$. For $N_\lambda \gg 1$, the size of these plateaus will be large enough for the synchronized clusters formed under conditions of small mismatches to depend weakly on the desynchronization action of the elements located in regions with large gradients of ω_j .

This is confirmed by comparing the dependences $\varepsilon(\Delta^*)$ obtained for disorder with filtered shortwave components and unfiltered disorder. For the specific series of disorder corresponding to Fig. 11, the spectra and the relevant dependences $\varepsilon(\Delta^*)$ are given in Fig 13. Random component of ω_j was filtered with the aid of a linear low-pass filter:

$$\omega_j = \Delta \frac{j - 1}{N - 1} + \Delta^* F[\xi_j],$$

where

$$F[\xi_j] = \frac{(\xi_{j-1} + \xi_j + \xi_{j+1})}{3}$$

acts as a filter of high harmonics. It is easy to show that the action of such a filter is equivalent to multiplication of the Fourier spectrum $S(k)$ by $f(k) = (1 + 2 \cos k)/3$. It is important that the shortwave components of spatial disorder weakly affect the value of energy ε . Therefore, it is actually demanded that the frequency distribution should have sufficiently extended plateaus “on the average” as it is illustrated in

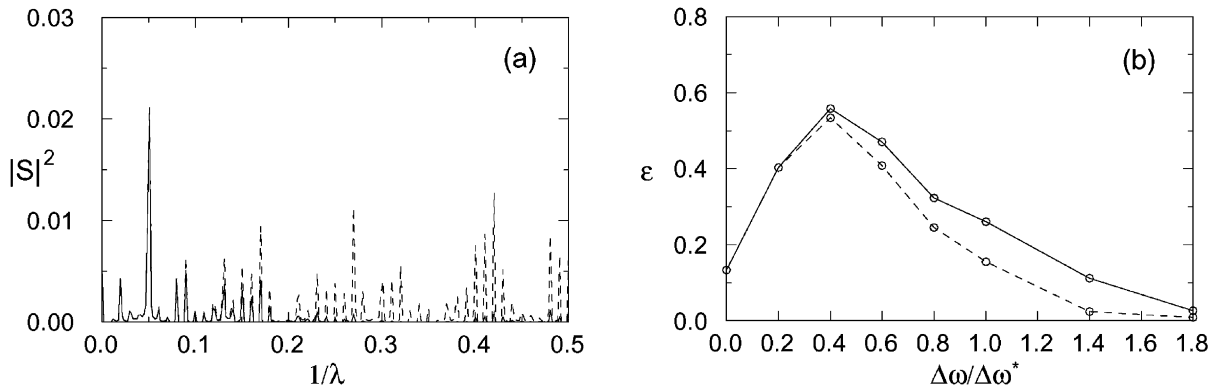


Fig. 13. (a) Power spectrum of the random component of ω_j depicted in Fig. 11 (dashed line) and of the filtered random component (solid line); (b) ε vs. relative disorder level, the same set of random numbers $\{\xi_j\}_{j=1}^N$ was used with different Δ^* . Solid line corresponds to filtered disorder, dashed line to the non-filtered one; $\Delta = 6.0$.

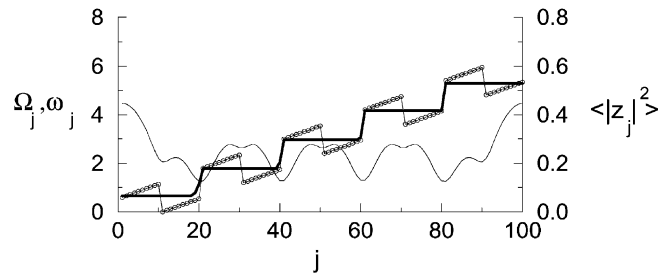


Fig. 14. Chain with a meander of magnitude Δ^* imposed on the linear frequency trend, $\Delta = 6.0$ and $\Delta^* = 0.2\Delta$. Time-averaged intensity profile $\langle |z_j|^2 \rangle$ (solid line), averaged frequencies of oscillations Ω_j (bold line), and natural frequencies ω_j (circles connected by dashed line) are presented.

Fig. 14. This figure presents the case of a distribution in which the frequency gradients of initial distribution are retained everywhere except at several points. Jumps at some points provide a nonmonotonic variation of the frequency and conservation of the total range of frequency scatter like in the case of their monotonic variation. With the mechanism described above taken into account, the optimal value of the frequency scatter Δ_{opt}^* in Figs. 12 and 13 becomes clear. It is due to the fact that a longwave component of sufficiently large amplitude can compensate the initial frequency gradient in the array.

3. Coupled homogeneous chains

This section will be devoted to consideration of coupled homogeneous chains of oscillators with oscillator death [34,35]. As a model we consider two coupled chains of self-excited oscillators whose dynamics in a quasiharmonic approximation is described by the following equations for the slowly varying complex amplitudes a_j and b_j :

$$\dot{a}_j = (p + i\Delta)a_j - (1 + \alpha)|a_j|^2 a_j + (d_1 + id_2)(a_{j+1} - 2a_j + a_{j-1}) + c(b_j - a_j), \quad (13)$$

$$\dot{b}_j = pb_j - |b_j|^2 b_j + d_1(b_{j+1} - 2b_j + b_{j-1}) + c(a_j - b_j), \quad (14)$$

for $j = 1, \dots, N$, with the boundary conditions $a_0 = a_1$, $a_{N+1} = a_N$, $b_0 = b_1$, and $b_{N+1} = b_N$ (free ends). Here, Δ and α describe the linear and nonlinear frequency mismatches of the oscillators, p is the growth rate, d_1 and d_2 are the coefficients of active and reactive coupling between elements in the chains, respectively, and c is the coefficient of coupling between chains. This is a fairly generic system, which probably has no direct relevance to experimental situations, but is a good model to study phenomena that can happen in Nature in general.

3.1. Mechanism of localized structure formation

We will mainly focus on localized structures with partially or completely synchronized oscillators [8]. One of the mechanisms responsible for the formation of such structures (adequately referred to as coherent structures) is associated with oscillator death. Due to this effect, the trivial equilibrium state is stable for sufficiently strong coupling c and large linear detuning Δ . At the same time, if the linear

detuning can be compensated by the nonlinear one ($\alpha|a_{jk}|^2 \approx \Delta$), then an equilibrium state with finite amplitudes is also stable within a certain range of parameters. For a homogeneous state, one can obtain

$$|a_j|^2 = |b_j|^2 = \Delta\alpha - 4(c - p) + \{[\Delta\alpha - 4(c - p)]^2 - 16(1 + \frac{1}{4}\alpha^2)[\frac{1}{4}\Delta^2 - c^2 - (c - p)^2]\}^{1/2} \times [4(1 + \frac{1}{4}\alpha^2)]^{-1}, \tag{15}$$

with

$$4c^2 - 4(c - p)^2 < \Delta^2 < 4c^2 - 4(c - p)^2 + [\frac{1}{2}\Delta\alpha - 2(c - p)]^2 (1 + \frac{1}{4}\alpha^2)^{-1}, \tag{16}$$

$$\Delta\alpha - 4(c - p) > 0.$$

One can naturally expect that, for certain limitations on the value of the coupling between the elements, states with $a_j = b_j = 0$ and $a_j = b_j \neq 0$ can coexist in both chains and thus form stationary fronts and localized structures.

Depending on the initial and boundary conditions and on external actions, these state may form patterns of various configurations.

Let us consider an elementary example of $d_2 = 0$ and define the initial amplitude distribution as a step function:

$$a_j^2 = b_j^2 = \begin{cases} (0.0, & j = 1, \dots, 50 \\ 0.72, & j = 51, \dots, 128 \end{cases}$$

(here $\Delta = 2$; $\alpha = 5.75$; $p = 0.5$; $c = 0.51$).

At weak coupling between the elements inside the array ($d_1 \ll d_{1cr} = 0.09$), a motionless front that separates the oscillators in excited and unexcited states is formed. At strong coupling ($d_1 > d_{1cr}$), the regime of oscillator death is prevailing, and the region in which it is realized broadens and embraces all the array. For $d_1 \gg d_{1cr}$, the front velocity V has the dependence on coupling parameter typical of critical phenomena: $V \sim \sqrt{d_1 - d_{1cr}}$, but makes a sharp (stepwise) transition from zero to nonzero velocities at $d_1 = d_{1cr}$.

Suppose that a localized excitation with amplitudes close to the stationary ones described by the expression (15) is defined at the initial moment of time. Then, at $d_2 = 0$, either localized structures are formed (if $d_1 > d_{1cr}$) or the excitations damp (if $d_1 < d_{1cr}$). The presence of a reactive component in the coupling coefficient $d_2 \neq 0$ in one of the chains provides for the existence of localized structures in the latter case too. The result will depend significantly on the sign of the product αd_2 . If $\alpha d_2 < 0$, i.e. when the corresponding Schrödinger equation describes self-compression of localized perturbation in the limit $\alpha \rightarrow \infty, d_2 \rightarrow \infty$, the damping is accelerated. In the opposite case ($\alpha d_2 > 0$), the result depends on the competition of two effects: the expansion of the region of oscillator death described above and the spreading, in the opposite direction, of localized excitation due to combined action of nonlinearity $\alpha|a|^2$ and “dispersion” d_2 . Let us consider possible results of such a competition on an example of the evolution of a localized perturbation with a high initial amplitude for $p = 0.5$; $d_1 = 0.3$; $c = 0.51$; $\Delta = 2.0$; $\alpha = 5.75$; and $N = 128$.

As the dispersion d_2 is increased at $\alpha d_2 > 0$, the propagation velocity of the fronts forming the localized structure decreases. At a certain critical value $d_1' \approx d_1 = 0.3$, the effect of oscillator death is balanced by nonlinear self-expansion of the perturbation, and a stable structure is formed. Its size grows as the dispersion d' increases and, eventually, when the second critical value $d_2'' \approx 0.9$ is attained, the

effect of self-expansion becomes predominant. This leads to delocalization of the excitation which finally embraces all the array.

The most interesting phenomena occur when the values of d_2 approach d_2'' . Within the framework of a rigorously symmetric problem ($a_i \equiv a_{128-i+1}, b_i \equiv b_{128-i+1}, i = 1, \dots, 64$), an almost stationary amplitude distribution $|a_j|, |b_j|$ is first formed from the homogeneous localized excitation for d_2 slightly smaller than the critical one. This amplitude distribution is retained at large intervals of dimensionless time of the problem ($\sim 10^3-10^4$). After that, for much shorter time (≈ 10), the structure (regions of high-intensity oscillations) abruptly expands symmetrically and then rapidly recovers its initial quasistationary amplitude distribution. Still further, this process is repeated. As d_2 is increased, the average repetition rate of such bursts increases. The time intervals between these events are random even in the absence of noise. Bursting structures in this case look like in the case of non-symmetric structures located at the boundary of the chains (see Fig. 15).

Additional forcing or perturbation of the initial conditions that break the symmetry with respect to the center of the chain do not change significantly the structure in the time intervals between the bursts. However, the structures shift in one or another direction at each burst. These shifts occur randomly, both

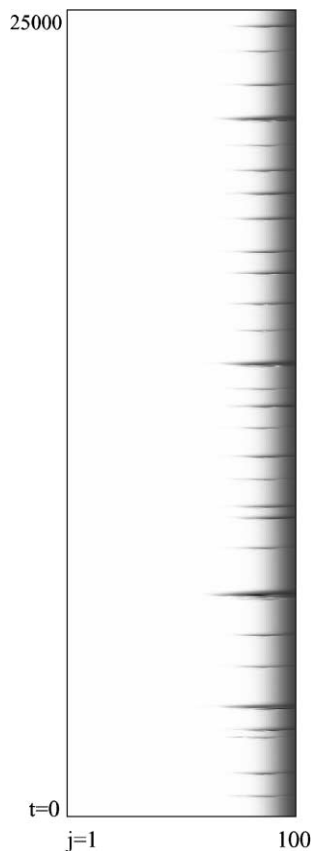


Fig. 15. Dependence of the oscillation intensity $|a_j(t)|^2$ on the element's position in the array j and time t (shading corresponds to the intensity).

at noise forcing and without it when the initial conditions are taken to be asymmetric. Random walk of the structure eventually leads it to the end of the chain. Thus, we naturally encounter the problem of a boundary layer in the considered chain of self-excited oscillators.

3.2. Nonpropagation to propagation transition via intermittency

Boundary layer structures formed as a result of the mentioned above “random walks” are very similar to free structures. Nevertheless, from the physical point of view another interpretation can be useful. Consider two semi-infinite coupled chains, with a boundary layer structure formed by some initial perturbation of several elements near the boundary at $t = 0$. In this case for zero value of reactive coupling ($d_2 = 0$) this initial excitation remains localized for any value of d_1 . Front propagation is possible only for sufficiently large values of the reactive coupling $d_2 > d_{2cr}$ ($d_{2cr} \approx 0.9$ for $p = 0.5$; $d' = 0.3$; $c = 0.51$; $\Delta = 2.0$; $\alpha = 5.75$). In certain domains of d_1 (in particular for $d_1 \approx 0.3$, which is used in the present paper) the transition from nonpropagation to propagation occur via intermittency.

An example of such a situation is given in Fig. 15. Again, one can see the intermittency in the dynamics of amplitudes of oscillators, when long laminar phases of constant amplitudes are interrupted by chaotic bursts. The number of bursts during the time interval $\Delta t = 50,000$ versus the value of reactive coupling d_2 is plotted in Fig. 16 for active coupling $d_1 = 0.302$. One can see two regions of intermittent behavior. The transition to intermittency in the left and right regions occurs after the loss of stability of a periodically oscillating structure with periodically modulated amplitudes of a and b (quasistationary mode) and of a stationary structure with constant amplitudes of a and b (stationary mode), respectively. The time series of the intensity of oscillations of one of the elements for d_2 from both intermittent regions are presented in Fig. 17.

In order to identify the bifurcations which lead to chaotic intermittent behavior in the system we employed two commonly used tools. First we have constructed a one-dimensional return map by taking local maxima in the observed time series $|a_{95}(t)|^2$. Fig. 18 shows the return maps for different values of coupling parameter d_2 for the transition from quasistationary mode to intermittency. Return maps have a quadratic-like form, which corresponds to the simplest map exhibiting type-I intermittency (according

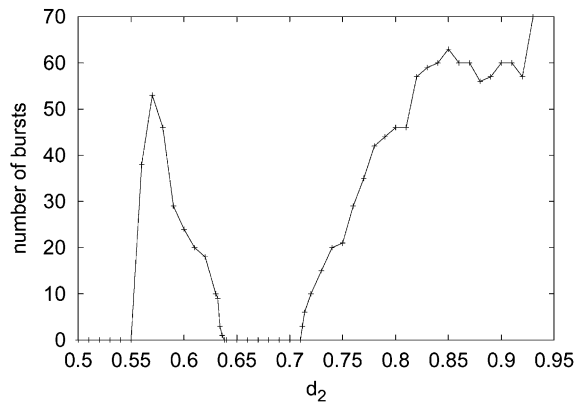


Fig. 16. Dependence of the number of bursts ([per time interval $\Delta t = 50,000$]) on the reactive coupling d_2 at $d_1 = 0.302$. For $d_2 > 0.93$, there are no intermittent bursts and front propagation is observed.

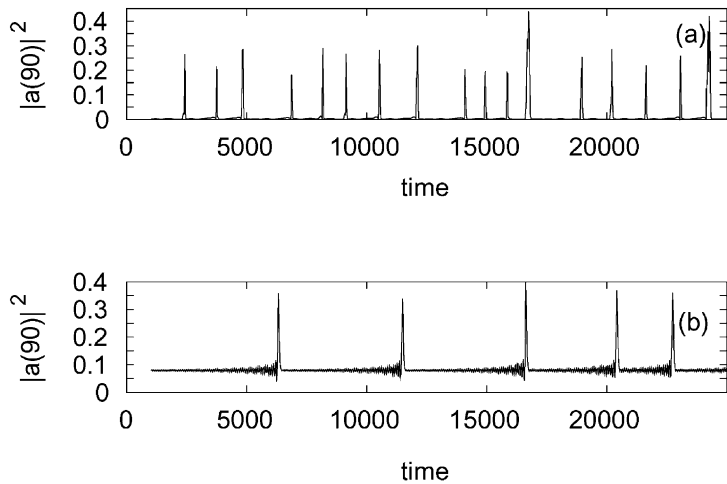


Fig. 17. Examples of time series showing intermittency. Intervals of laminar behavior are randomly interrupted by short bursts: (a) $d_2 = 0.56$, and (b) $d_2 = 0.72$.

to the classification by Pomeau and Manneville [36]) and which can be written in the form:

$$x_{j+1} = \varepsilon + x_j + x_j^2, \tag{17}$$

where ε is the distance from the bifurcation point, that depends on d_2 .

We have also calculated the statistical distribution of the laminar intervals. The results are represented by a histogram in Fig. 19. They show that this distribution has two maxima corresponding to minimal and maximal lengths of the laminar intervals. Such a distribution is the second good criteria of the existence of type-I intermittency. The peak in the region of long laminar intervals is less sharp than the one in the region of short laminar intervals. Such a distribution of laminar intervals lengths is usually observed

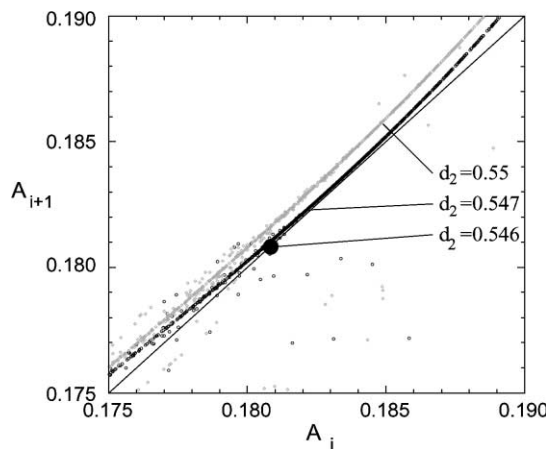


Fig. 18. The first return map constructed from the maxima of the time series of the intensity of oscillations of the 95th element for three different values of d_2 : $d_2 = 0.546$ —before bifurcation (stable attracting point), $d_2 = 0.547$ and $d_2 = 0.55$ —after bifurcation from quasistationary mode (quadratic-like map); and $d_1 = 0.3$.

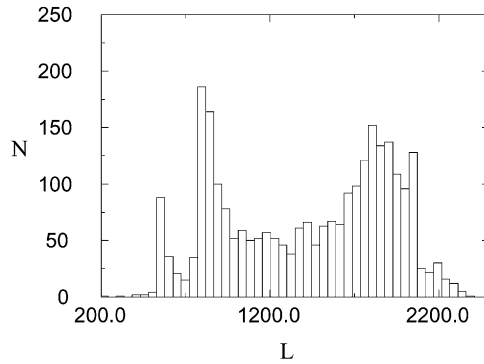


Fig. 19. Example of a histogram for the distribution of laminar intervals length for the 95th element after bifurcation from the quasistationary mode. Parameters: $d_1 = 0.3$, and $d_2 = 0.55$.

for type-I intermittency in the presence of noise [37]. In our $4N$ -dimensional system the role of such noise can be presumably played by some nonresonant modes, which become slightly excited above the bifurcation threshold d_2^* , but do not grow during intermittency.

The situation is quite different in the region where intermittency is born from a stationary mode. Return maps obtained from local maxima of time series of intensity and sample histogram are presented in Figs. 20 and 21, respectively. One can see that the return map is not one-dimensional strictly speaking. Our preliminary examination of the bifurcation suggests that the bifurcation can correspond to type-I intermittency (i.e. the Floquet multiplier crosses the unit circle at $+1$), but the return map has a high-order (for example, cubic) term with such a coefficient that this term is essential near the bifurcation point

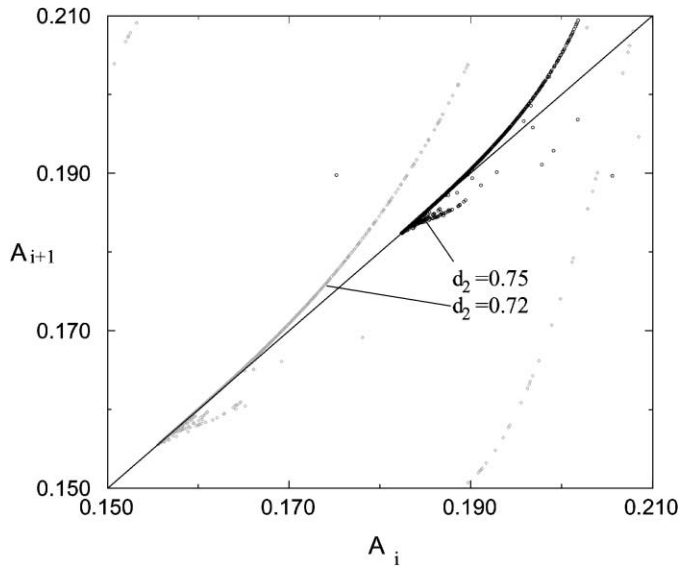


Fig. 20. The first return map constructed from the maxima of the time-series of the intensity of oscillations of the 95th element for two different values of d_2 after bifurcation from the stationary mode, $d_1 = 0.302$.

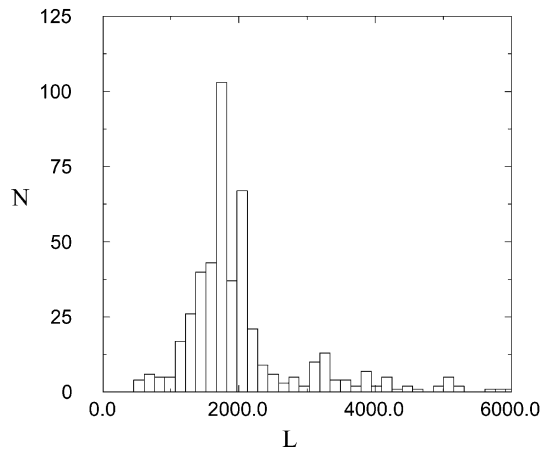


Fig. 21. Example of a histogram for the distribution of laminar interval length for the 95th element after bifurcation from the stationary mode. Parameters: $d_1 = 0.302$, and $d_2 = 0.75$.

(a similar map with essential cubic term was considered for example in [38]). Analysis of this bifurcation will be reported elsewhere.

Finally, we consider the action of external noise on the intermittent front dynamics considered above. We introduce an additive noise into our system (13) and (14) in the following fashion:

$$\begin{aligned} \dot{a}_j = & (p + i\Delta)a_j - (1 + \alpha)|a_j|^2 a_j + (d_1 + id_2)(a_{j+1} - 2a_j + a_{j-1}) \\ & + c(b_j - a_j) + \delta(\xi_1 + i\xi_2), \end{aligned} \tag{18}$$

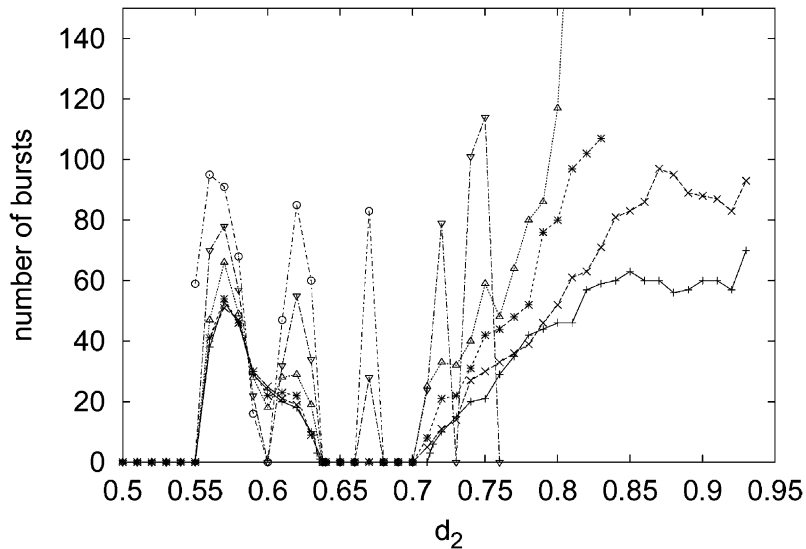


Fig. 22. The number of bursts per 5×10^4 times units in the system with noise (18)–(19) vs. d_2 , $d_1 = 0.302$. The amplitude of noise $\delta = 0$ (no noise, +), 0.0001 (x), 0.0005 (*), 0.001 (Δ), 0.002 (∇), and 0.003 (O). The curves break at the values of d_2 , where intermittency is replaced by pure propagation.

$$\dot{b}_j = pb_j - |b_j|^2 b_j + d_1(b_{j+1} - 2b_j + b_{j-1}) + c(a_j - b_j) + c(a_j - b_j) + \delta(\xi_3 + i\xi_4), \quad (19)$$

where ξ_k , $k = 1, 2, 3$, and 4 are random numbers uniformly distributed over $[-0.5; 0.5]$. The results of numerical simulation are presented in Fig. 22 (cf. Fig. 16). Quite naturally small-amplitude noise slightly alters the frequencies of bursting, but when the amplitude of the noise δ is increased, an unexpected phenomena can be observed. First, the frequency of chaotic bursting increases for some values of d_2 , and for intense noise ($\delta = 0.2$ and 0.3) chaotic bursting arises for such values d_2 , where bursting was not observed. But the most important observation is that the number of chaotic bursts decreases and even vanishes for certain domains of d_2 . Thus, noise can suppress chaotic intermittent bursting and provides a way to control the intermittent front dynamics.

4. Conclusion

We would like to conclude the paper with a few comments on the role of spatial and temporal irregularities in networks of dynamical elements. A traditional view is that chaos and/or disorder act in a destructive way. Many examples are known presently which provide the evidence of the opposite. We have already mentioned that disorder introduced into networks of oscillators can enhance synchronization and make chaotic dynamics regular [29–33]. Noise introduced into nonlinear dynamical systems can lead to nontrivial effects too. As a well-known example we can mention stochastic resonance [39–42]. Spatially uncorrelated noise can enhance stochastic resonance effects in the spatio-temporal variant [43,44], facilitate signal propagation in arrays of bistable systems [45,46], sustain traveling waves in subexcitable chemical media [47], sustain patterns (including the spiral ones) [48,49], induce pattern transitions [50] and fronts [51], and so on. In our paper we considered how disorder can induce formation of patterns (synchronized clusters) and increase the intensity of oscillations and how noise can suppress chaotic bursting in systems with oscillatory death. These effects can be considered as new examples of nontrivial action of noise in arrays of coupled oscillators.

Acknowledgements

This research was supported by the “Leading Scientific Schools of the Russian Federation” Program (Project 00-15-96582). G.V. Osipov was supported by the Russian Foundation for Basic Research (Project 99-02-17742).

References

- [1] M.I. Rabinovich, M.M. Sushchik, The regular and chaotic dynamics of structures in fluid flows, *Sov. Phys. Usp.* 33 (1990) 1–35.
- [2] M.C. Cross, P.C. Hohenberg, Pattern formation outside of equilibrium, *Rev. Mod. Phys.* 65 (1993) 851–1112.
- [3] V.S. Afraimovich, V.I. Nekorkin, G.V. Osipov, V.D. Shalfeev, *Synchronization, Structures and Chaos in Nonlinear Synchronization Networks*, World Scientific, Singapore, 1995.
- [4] R.E. Mirollo, S.H. Strogatz, Amplitude death in arrays of limit-cycle oscillators, *J. Stat. Phys.* 60 (1990) 245–262.
- [5] H.-A. Tanaka, A.I. Lichtenberg, S. Oishi, Self-synchronization of coupled oscillators with hysteretic responses, *Physica D* 100 (1997) 279–300.

- [6] L.O. Chua, T. Roska, The CNN paradigm, *IEEE Trans. Circuits Syst. I: Fundam. Theory Appl.* 40 (1993) 147–156.
- [7] G.V. Osipov, M.M. Sushchik, Coherent structures in coupled chains of self-excited oscillators, *Phys. Lett. A* 201 (1995) 205–212.
- [8] K. Bar-Eli, On the stability of coupled chemical oscillators, *Physica D* 14 (1985) 242–252.
- [9] K. Bar-Eli, Coupling of chemical oscillators, *J. Phys. Chem.* 88 (1984) 3616–3622.
- [10] Y. Yamaguchi, H. Shimizu, Theory of self-synchronization in the presence of native frequency distribution and external noises, *Physica D* 11 (1984) 212–226.
- [11] G.B. Ermentrout, Oscillator death in populations of “all-to-all” coupled nonlinear oscillators, *Physica D* 41 (1990) 219–231.
- [12] D.G. Aronson, G.B. Ermentrout, N. Koppel, Amplitude response of coupled oscillators, *Physica D* 41 (1990) 403–449.
- [13] P.C. Matthews, S.H. Strogatz, Phase diagram for the collective behavior of limit-cycle oscillators, *Phys. Rev. Lett.* 65 (1990) 1701–1704.
- [14] P.C. Matthews, R.E. Mirollo, S.H. Strogatz, Dynamics of a large system of coupled nonlinear oscillators, *Physica D* 52 (1991) 293–331.
- [15] M. Yoshimoto, K. Yoshikawa, Y. Mori, Coupling among three chemical oscillators: synchronization, phase death, and frustration, *Phys. Rev. E* 47 (1993) 864–874.
- [16] R. Herrero, M. Figueras, J. Ruis, F. Pi, G. Orriols, Experimental observation of the amplitude death effect in two coupled nonlinear oscillators, *Phys. Rev. Lett.* 84 (2000) 5312–5315.
- [17] Y. Kuramoto, *Chemical Oscillations, Waves and Turbulence*, Springer, Berlin, 1984.
- [18] G.V. Osipov, M.M. Sushchik, Synchronized clusters and multistability in arrays of oscillators with different natural frequencies, *Phys. Rev. E* 58 (1998) 7198–7207.
- [19] S.K. Sarna, In vivo myoelectric activity: methods, analysis and interpretation. In: *Handbook of Physiology. Section 6: The Gastrointestinal System*. S.G. Schultz, J.D. Wood, B.B. Rauner (Eds.), American Physiological Society, Bethesda, ND, 1989.
- [20] B.R. Noack, F. Ohle, H. Eckelmann, On cell formation in vortex streets, *J. Fluid Mech.* 227 (1991) 293–308.
- [21] L.L. Rubchinsky, M.M. Sushchik, Disorder can eliminate oscillator death, *Phys. Rev. E* 62 (2000) 6440–6446.
- [22] S.K. Sarna, E.E. Daniel, Y.I. Kinoma, Simulation of slow-wave electrical activity of small intestine, *Am. J. Physiol.* 221 (1971) 166.
- [23] D. Robertson-Dunn, D.A. Linkens, A mathematical model of the slow-wave electrical activity of the human small intestine, *Med. Biol. Eng.* 12 (1974) 750.
- [24] G.B. Ermentrout, N. Koppel, Frequency plateaus in a chain of weakly coupled oscillators, *SIAM J. Math. Anal.* 15 (1984) 215–237.
- [25] S.D. Drendel, N.P. Hors, V.A. Vasiliev, *Dynamics of Cell Populations*, Gorky University Press, Gorky, USSR, 1984, p.108 (in Russian).
- [26] V.A. Vasiliev, Yu.M. Romanovsky, V.G. Yakhno, *Autowave Processes*, Nauka, Moscow, 1987 (in Russian).
- [27] G.B. Ermentrout, W.C. Troy, The uniqueness and stability of the rest state for strongly coupled oscillators, *SIAM J. Math. Anal.* 20 (1989) 1436–1446.
- [28] G.V. Osipov, M.M. Sushchik, The effect of natural frequency distribution on cluster synchronization in oscillator arrays, *IEEE Trans. Circuits Syst. I: Fundam. Theory Appl.* 44 (1997) 1006–1010.
- [29] Y. Braiman, W.L. Ditto, K. Wiesenfeld, M.L. Spano, Disorder-enhanced synchronization, *Phys. Lett. A* 206 (1995) 54–60.
- [30] N. Mousseau, Synchronization by disorder in coupled systems, *Phys. Rev. Lett.* 77 (1996) 968–971.
- [31] Y. Braiman, J.F. Lindner, W.L. Ditto, Taming spatiotemporal chaos with disorder, *Nature* 378 (1995) 465–467.
- [32] J.F. Lindner, B.S. Prusha, K.E. Klay, Optimal disorders for taming spatiotemporal chaos, *Phys. Lett. A* 231 (1997) 164–172.
- [33] A. Gavrielides, T. Kottos, V. Kovanis, G.P. Tsironis, Spatiotemporal organization of coupled nonlinear pendula through impurities, *Phys. Rev. E* 58 (1998) 5529–5534.
- [34] G.V. Osipov, M.M. Sushchik, Mechanism of localized structure formation in coupled chains of self-oscillators, *Izv. Vu Zov. Prikladnaya Nelineinaya Dinamika* 2 (1994) 24–29 (in Russian).
- [35] G.V. Osipov, M.M. Sushchik, Self-structures and rhythms in coupled arrays of oscillators, *Bull. Russ. Acad. Sci., Phys. Vibr. (Phys. Suppl.)* 61 (1997) 41–45.
- [36] Y. Pomeau, P. Manneville, Intermittent transition to turbulence in dissipative dynamical systems, *Commun. Math. Phys.* 74 (1980) 189–197.
- [37] J.F. Hirsch, B.A. Huberman, D.J. Scalpiano, Theory of intermittency, *Phys. Rev. A* 25 (1982) 519–532.
- [38] S.C. Venkataramani, B.R. Hunt, E. Ott, Bubbling transition, *Phys. Rev. E* 54 (1996) 1346–1360.

- [39] K. Wiesenfeld, F. Moss, Stochastic resonance and the benefits of noise: from ice ages to crayfish and SAUIDS, *Nature* 373 (1995) 33–36.
- [40] A.R. Bulsara, L. Gammaioni, Tuning in to noise, *Phys. Today* 49 (1996) 39–45.
- [41] L. Gammaioni, P. Haggi, P. Jung, F. Marchesoni, Stochastic resonance, *Rev. Mod. Phys.* 70 (1998) 223–287.
- [42] V.S. Anishchenko, A.B. Neiman, F. Moss, L. Schimansky-Geier, Stochastic resonance: Noise enhanced order, *Phys. Usp.* 42 (1999) 7–36.
- [43] J.F. Lindner, B.K. Meadows, W.L. Ditto, M.E. Inchiosa, A.R. Bulsara, Scaling laws for spatiotemporal synchronization and array enhanced stochastic resonance, *Phys. Rev. E* 53 (1996) 2081–2086.
- [44] M. Locher, G.A. Johnson, E.R. Hunt, Spatiotemporal stochastic resonance in a system of coupled diode resonators, *Phys. Rev. Lett.* 77 (1996) 4698–4701.
- [45] J.F. Lindner, S. Chandramouli, A.R. Bulsara, M. Locher, W.L. Ditto, Noise enhanced propagation, *Phys. Rev. Lett.* 81 (1998) 5048–5051.
- [46] M. Locher, D. Cigna, E.R. Hunt, Noise sustained propagation of a signal in coupled bistable electronic elements, *Phys. Rev. Lett.* 80 (1998) 5212.
- [47] S. Kadar, J. Wang, K. Showalter, Noise-supported traveling waves in sub-excitable media, *Nature* 391 (1998) 770–772.
- [48] P. Jung, G. Mayer-Kress, Spatiotemporal stochastic resonance in excitable media, *Phys. Rev. Lett.* 74 (1995) 2130–2133.
- [49] H. Hempel, L. Schimansky-Geier, J. Garcia-Ojalvo, Noise-sustained pulsating patterns and global oscillations in subexcitable media, *Phys. Rev. Lett.* 82 (1999) 3713–3716.
- [50] H. Zhonghuai, Y. Lingfa, X. Zuo, X. Houwen, Noise induced transition and spatiotemporal stochastic resonance, *Phys. Rev. Lett.* 81 (1998) 2854–2857.
- [51] M.A. Santos, J.M. Sancho, Noise-induced fronts, *Phys. Rev. E* 59 (1999) 98–102.